Modulation of Pre- and Postsynaptic Calcium Dynamics by Ionotropic Glutamate Receptors at a Plastic Synapse

Neil E. Schwartz and Simon Alford

JN 79:2191-2203, 1998.

Journal of Neurophysiology publishes original articles on the function of the nervous system. It is published 12 times a year (monthly) by the American Physiological Society, 9650 Rockville Pike, Bethesda MD 20814-3991. ISSN: 0022-3077, ESSN: 1522-1598. Visit our website at http://www.the-aps.org/.

Modulation of Pre- and Postsynaptic Calcium Dynamics by Ionotropic Glutamate Receptors at a Plastic Synapse

NEIL E. SCHWARTZ [1] AND SIMON ALFORD [1,2]
[1]*Department of Physiology and* [2]*Northwestern University Institute for Neuroscience, Northwestern University Medical School, Chicago, Illinois 60611*

Schwartz, Neil E. and Simon Alford. Modulation of pre- and postsynaptic calcium dynamics by ionotropic glutamate receptors at a plastic synapse. *J. Neurophysiol.* 79: 2191–2203, 1998. This study was conducted to assess the role of ionotropic glutamate receptors in the modulation of calcium dynamics on both sides of a vertebrate plastic synapse. Retrograde labeling of neuronal elements with high-affinity calcium-sensitive dyes was used in conjunction with confocal imaging techniques in an in vitro lamprey brain stem preparation. A prolonged calcium transient was measured both pre- and postsynaptically in response to a period of high-frequency (''tetanic'') stimulation to the vestibulospinal-reticulospinal synapse. The ionotropic glutamate receptor antagonists 6-cyano-7-nitroquinoxaline-2,3-dione (10 μM) and D,L−2-amino-5-phosphonopentanoate (D,L-AP5; 100 μM) reduced the calcium signal in both compartments of the synapse. The presynaptic D,L-AP5–sensitive component was enhanced markedly by the removal of Mg^{2+} from the superfusate. Increasing the extracellular stimulus intensity progressively augmented the presynaptic calcium signal, suggesting the recruitment of excitatory axo-axonic inputs onto these fibers. Further, the presence of an excitatory amino acid-mediated presynaptic potential underlying a component of the Ca^{2+} signal was demonstrated by electrophysiological recordings from vestibulospinal axons. Bath application of agonist, in the presence of tetrodotoxin (1 μM), confirmed the existence of *N*-methyl-D-aspartate receptors at the presynaptic element capable of modulating calcium levels. The postsynaptic Ca^{2+} response, which is known to be necessary for long-term potentiation (LTP) induction at this synapse, was localized to areas of the dendritic tree that correlated with the location of known synaptic inputs; thus the synaptically activated rise in postsynaptic calcium may confer the synapse specificity of LTP induction previously demonstrated. In summary, we have demonstrated the existence of physiologically activated presynaptic ionotropic glutamate receptors that are capable of modulating levels of intracellular calcium and have highlighted the importance of receptor-mediated increases in postsynaptic calcium for neuronal plasticity in the lamprey.

INTRODUCTION

Transient rises in intracellular Ca^{2+} appear necessary for the induction of long-term potentiation (LTP), the major experimental paradigm for the study of mechanisms underlying learning and memory (Bliss and Collingridge 1993; Bliss and Lømo 1973). Although much effort is focused on the mammalian hippocampus, LTP occurs throughout the neuraxis, from cortex (Iriki et al. 1989; Kimura et al. 1989) to spinal cord (Pockett and Figurov 1993; Randic et al. 1993) in a variety of species. Excitatory amino acid receptors, particularly those of the *N*-methyl-D-aspartate (NMDA) subclass are thought to act as Ca^{2+} ionophores in the LTP induction process (Alford et al. 1993; Bliss and Collingridge 1993; Collingridge et al. 1983; Lynch et al. 1983; Malenka and Nicoll 1993). However, a key outstanding issue is the role of the presynaptic cell in plasticity; unfortunately, the limiting size of the mammalian terminal renders it difficult to study directly.

Lamprey reticulospinal neurons of the posterior rhombencephalic reticular nucleus (PRRN) provide descending drive to the spinal cord (Buchanan et al. 1987; Ohta and Grillner 1989). Vestibulospinal axons from the two vestibular nuclei, the nucleus octavomotorii intermediate (nOMI) and posterior (nOMP) make en passant synapses (Deliagina et al. 1992a,b; Orlovsky et al. 1992; Rovainen 1979) onto the dendrites of reticulospinal neurons and contain a chain of presynaptic elements along their length (Rovainen 1979; see also Shupliakov et al. 1992). The synapse is glutamatergic comprising α-amino-3-hydroxy-5-methyl-4-isoxazolepropionate (AMPA), NMDA, and electrical components (Alford and Dubuc 1993). The mechanisms underlying fast excitatory synaptic transmission are similar to those elucidated in the lamprey spinal motor system (Alford and Grillner 1990; Buchanan et al. 1987; Dale and Grillner 1986) and other vertebrate synapses (Collingridge and Lester 1989).

This synapse undergoes robust pathway-specific LTP in response to high-frequency stimulation of vestibulospinal axons (Alford et al. 1995). Potentiation is blocked by postsynaptic Ca^{2+} chelation, suggesting a role for Ca^{2+} signaling in its induction. This, however, does not preclude the involvement of the presynaptic terminal. There is evidence from other vertebrate preparations that presynaptic mechanisms may be necessary for LTP expression (e.g., Bekkers and Stevens 1990; Kullmann and Nicoll 1992; Malinow and Tsien 1990). In the simplest case, Ca^{2+} entry through voltage-operated Ca^{2+} channels (VOCCs), in addition to precipitating exocytosis, could begin a cascade of cellular events leading to enhanced release. Such a mechanism has been proposed at the hippocampal mossy fiber-CA3 synapse, for example (Nicoll and Malenka 1995). Further, there exists a possible role for ''retrograde messengers'' in affecting presynaptic loci (O'Dell et al. 1991; Stevens and Wang 1993; Williams et al. 1989), or the activation of autoreceptors.

In this study, we have used microfluorimetry to investigate the control of Ca^{2+} fluxes by ionotropic glutamate receptors in presynaptic vestibulospinal axons and postsynaptic reticulospinal dendrites. The large neuronal elements and the optical clarity of the tissue provides excellent resolution of Ca^{2+} signals in an intact vertebrate brain and also allows for direct

0022-3077/98 $5.00

electrophysiological recording from the presynaptic compartment. Portions of this material have been reported in abstract form (Schwartz et al. 1995, 1996).

METHODS

In vitro lamprey brain stem preparation

Experiments were performed on the isolated brains of larval (ammocœte) lampreys, *Petromyzon marinus*, in accordance with local and national guidelines. The animals were anesthetized with tricaine methanesulfonate (MS222; Sigma, St. Louis, MO), decapitated, and dissected in a cold saline solution (Ringer) of the following composition (in mM): 86 NaCl, 2.1 KCl, 2.6 $CaCl_2$, 1.8 $MgCl_2$, 4 glucose, and 26 $NaHCO_3$; bubbled with 95% O_2-5% CO_2 to a pH of 7.4 (modified from Wickelgren 1977). The skin, musculature, braincase, and choroid plexus were removed; the obex was opened up and the optic tectum/cerebellum removed, fully exposing the basal and alar plates of the fourth ventricle. The tissue was placed dorsal surface upward in a cooled ~500 μl chamber with a cover-slip floor that was inserted onto the stage of an inverted Nikon Diaphot microscope. The recording chamber was continually superfused with cold oxygenated Ringer solution (8–10°C) or solutions of pharmacological agents bath-applied at a perfusion rate of 1 ml/min.

Retrograde labeling of brain stem

Dye filling of the brain stem was achieved by the 16–22 h application of the dextran-amine conjugates of calcium-sensitive dyes (McClellan et al. 1994) or dyes used for anatomic labeling [3,000 or 10,000 molecular weight (MW) Calcium Green-1, 10,000 MW Oregon Green 488 bis-(*o*-aminophenoxy)-*N*,*N*,*N*′,*N*′-tetraacetic acid (BAPTA)-1 or lysine-fixable fluorescein; Molecular Probes, Eugene, OR]. Dye (5 mM) was applied by the internal perfusion of a glass pipette into which the cut end of the spinal cord (2–3 mm caudal to the obex) was drawn via suction. The perfusion apparatus consisted of a 10 μl syringe (Hamilton, Reno, NV) attached via thin tubing to one of two ports of a patch pipette holder, which in turn was connected to a short segment of silica tubing drawn to a thin tip and inserted within 50 μm of the distal tip of the glass pipette. Because dextran-conjugated dyes are only taken up into recently cut axons, the dye was injected into the pipette within 1 min of the cord being cut (Fig. 1*A*). As both vestibulospinal and reticulospinal axons project into the spinal cord, both pre- and postsynaptic elements of the vestibulospinal-reticulospinal synapse can be retrogradely labeled. Furthermore, segregation of the tracts in the spinal cord affords a means of selectively labeling either one compartment or the other of the synapse. Reticulospinal axons of the PRRN run in the lateral funiculi of the spinal cord; vestibulospinal tracts are found more medially (Rovainen 1974). Specific labeling of vestibulospinal axons was achieved by making partial cuts through the lateral aspects of the cord and allowing the axons time to reseal (~30 min). After this period, a full transection was made more caudally, and the dye applied in the preceding manner, ensuring that only the medial tracts would take up the dye (Fig. 1*B*). Selective reticulospinal labeling was achieved by making a partial cut through three-fourths of the spinal cord, leaving the lateral tracts in one hemicord intact. After allowing the axons time to reseal, a full transection was made more caudally and the dye applied, ensuring that only the lateral tracts would be filled (Fig. 1*C*). Preparations were superfused with cold oxygenated Ringer solution throughout the labeling period.

Confocal microscopy

Imaging was accomplished with a confocal laser scanning microscope (Bio-Rad MRC-600, Bio-Rad) using the 488 nm line of an argon ion laser as the excitor source. A fluorescein filter set was used with a ×20 (0.75NA) objective. Low-speed (2 Hz) imaging of axons and/or dendrites was carried out with a series of 16 image frames acquired before, during, and after a stimulus. Image analysis was performed using NIH Image (v.1.60/ppc). Identifiable axons or dendrites were either manually outlined or selected using the thresholding or density slice features. An automated search macro was used to analyze the identical size region in all subsequent image frames of the trial; the macro optimized the mean intensity within the defined region of interest within 11 pixels of the initial location in either dimension. Increases in fluorescence intensity (ΔF) were normalized to the first three or four frames (prestimulus), giving a baseline value of $\Delta F/F = 1.00$. Throughout the text all levels of significance are from one-tailed Student's *t*-tests expressed as a probability, P, that the results are from the same population. Errors are expressed as standard errors of the mean, which are normalized to the control (predrug) response for pharmacology experiments. A repetitive line scan (≤500 Hz) over a single area was used for high-speed imaging. For time series experiments (those in which agonists were washed into the bath), images were acquired at 0.067 Hz for the control and wash-out periods and 0.2 Hz during the drug application; the Kalman filter was used with two scans per image. All images were acquired with Bio-Rad software and three-dimensional reconstructions of image slices from multiple *z* planes were performed with a Silicon Graphics Indigo 2 computer using Voxel View software (Vital Images). Extracellular stimulations were achieved with tungsten electrodes (impedance = 0.5–2.0 MΩ) activated via a stimulus isolation unit. The location within the brain stem of vestibulospinal inputs from the nOMI and nOMP onto reticulospinal cells of the PRRN has been established previously using anatomic and electrophysiological techniques. Responses within a single PRRN cell to extracellular stimuli applied to various loci on the basal and alar plates has been determined systematically (Alford et al. 1995). Stimulus trains (tetani) were given at 50 Hz for 1 s (1.0 ms/stimuli) except where noted.

Electrophysiology

Electrophysiological recordings were from vestibulospinal axons of the nOMI or nOMP. Recordings used sharp microelectrodes filled with 3 M KCl; tip resistances were 30–50 MΩ. Data was observed, stored, and analyzed on a personal computer. Recording techniques were conventional and performed in current-clamp bridge mode with an Axoclamp-2A amplifier controlled with pClamp software (v.6.0.1; Axon Instruments, Foster City, CA). For some experiments, vestibulospinal axons were filled via pressure ejection with 0.5% dextran-conjugated fluorescein after recordings were made. The tissue was fixed in 4% formaldehyde, dehydrated with ethanol, and cleared with methyl salicylate. Imaging was performed as described in the previous section.

Drugs

All drugs were bath-applied in Ringer solution at a rate of 1 ml/min. CNQX, D,L-AP5, NMDA, and AMPA were obtained from Tocris Cookson (St. Louis, MO). Tetrodotoxin (TTX) was obtained from Sigma. Cyclothiazide was obtained from RBI (Natick, MA).

RESULTS

Dye concentration is low in retrogradely labeled neuronal processes

Retrograde labeling of reticulospinal and vestibulospinal axons, together and separately, was achieved with dex-

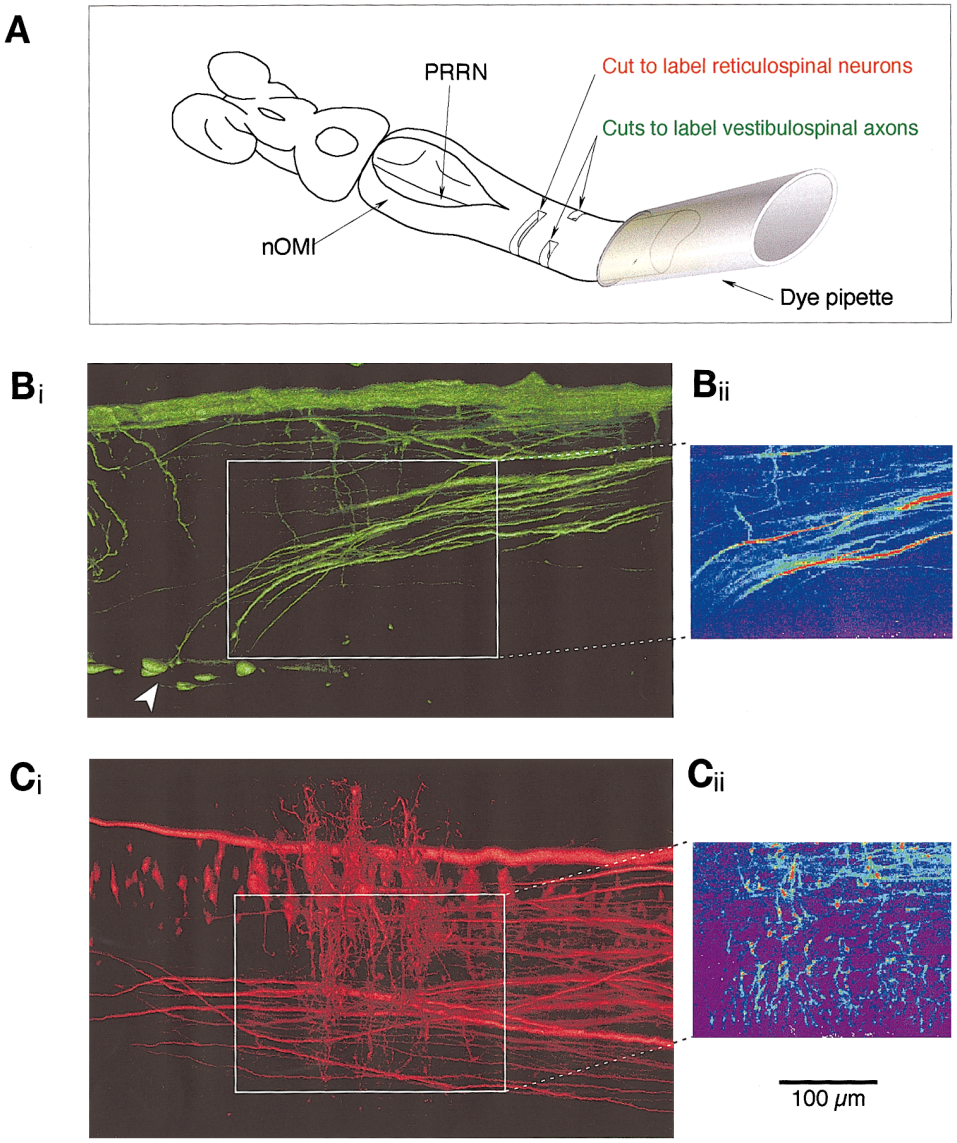

FIG. 1. Retrograde labeling of reticulospinal and vestibulospinal neurons in the brain stem. *A*: schematic showing the technique used for the retrograde labeling experiments. Cut spinal cord was exposed to dextran-conjugated lysine-fixable fluorescein dye (5 mM) in a suction pipette and maintained overnight in cold oxygenated Ringer solution. Selective loading of the postsynaptic reticulospinal neurons of the posterior rhombencephalic reticular nucleus (PRRN) was achieved by making a cut through the spinal cord to leave only the lateral funiculi intact. For selective loading of the presynaptic vestibulospinal axons and the nucleus octavomotorii intermediate (nOMI), the lateral funiculi were cut leaving only the medial tracts intact. *Bi*: reconstruction from multiple *z* planes of a retrograde fill of the medial tracts, showing the vestibulospinal axons and the nOMI (arrowhead). *Bii*: confocal optical section of the region investigated in this structure taken from within the boxed area of *Bi*. *Ci*: reconstruction from multiple *z* planes of a retrograde fill of the lateral funiculi, showing the reticulospinal neurons of the PRRN and their dendritic trees. Note that the axons seen coursing through the dendritic region parallel to the midline are from nonvestibular descending systems and are not of interest to these studies; further, these axons are in a plane of section far more dorsal than the vestibulospinal axons. *Cii*: confocal optical section of the region investigated in this structure taken from within the boxed area of *Ci*. Scale bar refers to all the anatomic data.

tran-conjugated dyes. This allowed for the loading of a number of presynaptic (vestibulospinal) and/or postsynaptic (reticulospinal) elements of the synapse of interest. Control experiments were carried out to determine the intracellular dye concentration achieved with the retrograde labeling technique as well as the lack of saturation of presynaptic Ca^{2+} signals. Spatially fixed because of their binding to endogenous proteins, the dextran-conjugated dyes are less likely to break down spatial Ca^{2+} gradients. Another important advantage of these dyes is that their large size precludes their entry into intracellular organelles (Schlatterer et al. 1992), giving a more accurate representation of free cytosolic calcium concentration ($[Ca^{2+}]_i$). However, a limitation of the retrograde labeling technique is the need to separately ascertain the concentration of dye achieved in the cells. Comparison of the dextran-conjugated fluorescein signal intensity in retrogradely labeled preparations to the intensity achieved with known quantities of the same dye in a patch electrode placed adjacent to a dye-loaded axon was used to determine the approximate intracellular dye concentration obtained within the axon. This technique ensured that the optical path length used to visualize the axon was very close to that used to visualize the control dye in the electrode. For these experiments axons were back-filled with 10,000 MW dextran-conjugated fluorescein. The axons subsequently were identified in the confocal microscope in unfixed live tissue. Patch electrodes containing the same dye then were positioned in the tissue and imaged in the same plane as the labeled axon. The results of these experiments demonstrate that an intracellular dye concentration of ~2 μM is achieved with the retrograde labeling technique (Fig. 2*A*).

Summation of calcium responses indicates a lack of dye saturation

Neurotransmitter release is thought to occur after a very rapid (200 μs) Ca^{2+} influx that transiently raises $[Ca^{2+}]_i$ to high levels (perhaps 200–300 μM) in the immediate vicinity

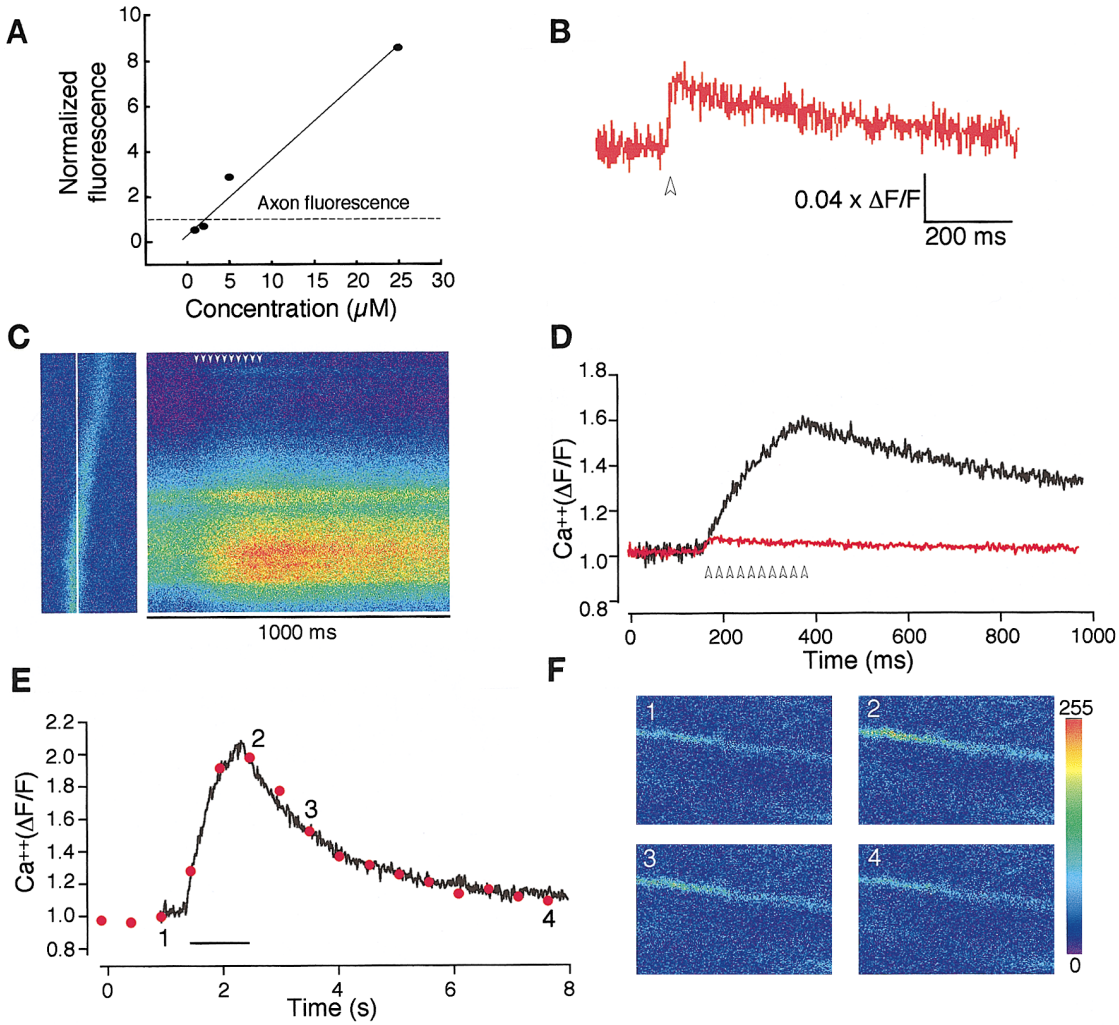

FIG. 2. A low non-saturating dye concentration is achieved with the retrograde labeling technique. *A*: comparison of dye fluorescence in a retrogradely labeled axon to a patch pipette filled with known concentrations of the same dye. Vestibulospinal axons were retrogradely labeled with dextran-conjugated fluorescein. Fluorescence intensity was given an arbitrary value of 1.0. Serial concentrations (in μM: 1, 2, 5, and 25) of the same dye were included in a patch pipette placed within the same tissue adjacent to the labeled axons with the same optical path. Graph suggests a dye concentration of $\sim$2 μM is achieved within the cells when the retrograde labeling technique is employed. *B*: high-speed scan of a single vestibulospinal axon. A high-frequency (500 Hz) line scan was made along the vertical line in the axon in *C* while a single stimulus (arrowhead) was given. *C*: location of the scanned line on the axon (*left*; axon was retrogradely labeled with Oregon Green 488 BAPTA-1 dextran), and the intensity of the fluorescence measured during line scanning (*right*). Line scanned from *bottom* to *top* of this trace in 2 ms (500 Hz), and the repeated scans are shown from *left* to *right* during 1 s. *D*: red trace is the same as in *B* but scaled in the *y* axis. Black trace is a similar scan of the same axon shown in *C* but during 10 stimuli at 50 Hz (stimulus timing shown by the arrowheads). *E*: In black, the response of the same axon shown in *C* to 50 stimuli at 50 Hz. Red circles plot the intensity of the response averaged over the axon when frames of data (192 $\times$ 128 pixels) were sampled at 2 Hz. Duration of this tetanic stimulus (1 s) is shown by the horizontal bar. Frames from the numbered points in *E* are shown in *F*. *F*: images of a vestibulospinal axon retrogradely-labeled with Oregon Green 488 BAPTA-1 dextran given a tetanic stimulus (bar in *E*). Intensity and timing of the axonal calcium signals corresponding to the frame numbers is shown graphically in *E*. Each frame is 79 μm in width. Midline is toward the *top;* rostral is toward the *left.* All images are pseudocolored to the scale shown in *F*.

of the Ca^{2+} ionophores responsible for its entry (Augustine et al. 1991; Llinas et al. 1992). For the experiments in this study, laser-scanning confocal microscopic images were acquired at rates of 2–500 Hz. Even at the fastest scanning frequencies, it is not possible to accurately measure Ca^{2+} that enters the cell with each action potential and is directly responsible for transmitter exocytosis. Furthermore, the high Ca^{2+} affinities of the dyes (K_d = 170–540 nM) (Eberhard and Erne 1991), which would be saturated by the large local concentrations of Ca^{2+} at the membrane adjacent to putative release sites, precludes the direct measurement of this immediate Ca^{2+} transient. Hence, the dye affinities and rates of scanning used in these experiments do not allow for the measurement of presynaptic Ca^{2+} transients that lead to transmitter release at the synaptic terminal. Rather, we have used these techniques to measure the relative magnitudes of Ca^{2+} levels reached during and shortly after ($\leq$5.5 s) a tetanic electrical stimulation, comparing experimental protocols in the same tissues. As an essential

control, it was necessary to determine if a true reflection of $[Ca^{2+}]_i$ is revealed by studying the fluorescence changes in this manner with these dyes. Stimuli were delivered extracellularly to selectively labeled calcium-sensitive dye-filled vestibulospinal axons, and fluorescence transients were measured with single high-frequency line scans (125–500 Hz). Various axonal stimulation protocols (5.5–75.0 μA; 50 Hz; 1.0 ms/stimulus) were used with the number of stimuli ranging from 1 to 50. Figure 2*B* shows a representative line scan of a vestibulospinal axon that was retrogradely-labeled with Oregon Green 488 BAPTA-1 dextran. The line through the axon shown in Fig. 2*C* was scanned at 500 Hz during the tetanus. Single stimuli applied to the axons resulted in a Ca^{2+} transient with a rate of rise not resolved at a 500-Hz recording frequency. Fifty hertz stimulation caused a summation of Ca^{2+} concentration in the axons such that 10 shocks markedly increased the amplitude of the transient (Fig. 2, *C* and *D*). Tetanic stimuli of 50 shocks for 1 s routinely were used in this study to mimic conditions in which LTP of outputs from these axons occurs. In the same axons, the response to such a stimulation was larger than for 10 shocks. In all cases where this was tested, fluorescence responses summed with progressively larger numbers of stimuli of a given amplitude ($n = 18$), suggesting a lack of saturation of the dyes. Recording of this tetanic stimulus induced rise in Ca^{2+} using a sequence of 16 128 × 92 pixel frames sampled at 2 Hz revealed substantially the same response (Fig. 2, *E* and *F*). The slower frame data accurately recorded this transient; this technique was used in the remainder of the study for two reasons: first, more complete spatial information could be obtained and second, the low-frequency recording technique was found to be much less likely to bleach the fluorescent dye. In general, the peak response for a given number of stimuli occurred at the termination of the tetanus, and in all cases the axonal Ca^{2+} transient outlasted the duration of the stimulus.

Pre- and postsynaptic calcium responses to tetanic stimulation

Dextran-conjugated calcium-sensitive dyes and low-frequency (2 Hz) confocal imaging were used to measure the Ca^{2+} signals on both sides of the synapse in response to a tetanic input. The tetanus used for these studies (50 Hz for 1 s) has been demonstrated to cause LTP of this synapse (Alford et al. 1995). Routinely, the ''peak'' response during the tetanus (which usually occurred at its termination) and the ''tail'' response at the end of the trial were used for analysis. The presynaptic tail response represents a measure of the Ca^{2+} signal after termination of the stimulus that will not be dominated by the high transients that result from presynaptic action potentials. Figure 3*A* shows an example of a typical experiment with both axons and dendrites present in the same visual field. The vestibular axons of the nOMI are identifiable as linear structures passing horizontally or diagonally across the field of view, whereas the PRRN reticulospinal dendrites can be seen as punctate or short linear segments aligned perpendicular to the axons. A tetanic input (50 Hz for 1 s; 1.0 ms/stimulus) was given to the vestibular axons of the ipsilateral nOMI, resulting in large Ca^{2+} transients both pre- and postsynaptically (Fig. 3, *A* and *B*). In this case, a peak $\Delta F/F$ of 1.81 in the axon and 2.78 in the dendrites was measured. On termination of the tetanus, the Ca^{2+} level slowly returned to baseline; the tail fluorescence (as observed 5.5 s after the stimuli ended) was 1.39 in the axon and 1.41 in the dendrites. The mean peak value fluorescence ($\Delta F/F$) obtained during the tetanus of the vestibulospinal axons was 2.02 ± 0.11 (mean ± SE; Fig. 3*C; n* = 21). After the termination of the tetanus, there was a slow decay in the fluorescence to baseline with a mean tail $\Delta F/F$ of 1.28 ± 0.06 (Fig. 3*C; n* = 21). Recording of PRRN reticulospinal dendrites during tetanic stimulation revealed a mean peak $\Delta F/F$ of 3.68 ± 0.74 and a tail response of 1.33 ± 0.09 (Fig. 3*C; n* = 13). The decay of these responses to baseline was slightly faster than recordings from axons of lamprey motoneurons after a single shock (Bacskai et al. 1995), although those recordings were not made from presynaptic elements.

Effect of CNQX and D,L-AP5 on calcium transients

Pharmacological agents were used in conjunction with Ca^{2+} imaging to examine the role of ionotropic glutamate

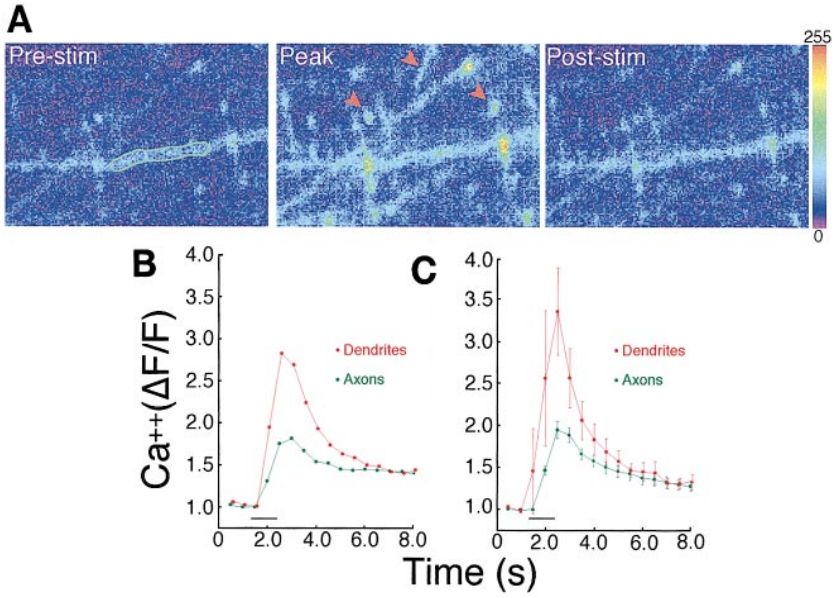

FIG. 3. Stimulation of vestibulospinal axons affects calcium homeostasis pre- and postsynaptically. *A*: pseudocolor confocal image of vestibulospinal axons (e.g., outlined in green) and reticulospinal dendrites (e.g., red arrowheads) retrogradely labeled with Calcium Green-1 dextran. Images were acquired at 2 Hz for 8 s for a total of 16 frames per trial. A tetanus (10 μA; 50 Hz for 1 s; 1.0 ms/stimulus) was applied to the vestibulospinal pathway. Pre-stim, resting state (mean of *frames 1* and *2*); peak, peak response to tetanus (mean of *frames 5* and *6*); post-stim, region 5.0–5.5 s after the tetanus (mean of *frames 15* and *16*). Midline is toward the *top;* rostral is toward the *left.* Each frame is 79 μm in width. The 256-color lookup table is shown to the *right,* with low $[Ca^{2+}]_i$ being blue and high $[Ca^{2+}]_i$ being red. *B*: graphic representation of the axonal and dendritic calcium response shown in *A*. Bar represents the 1 s tetanus. *C*: pooled results from axons ($n = 21$) and dendrites ($n = 13$). Error bars are SE; bar represents the 1-s tetanus.

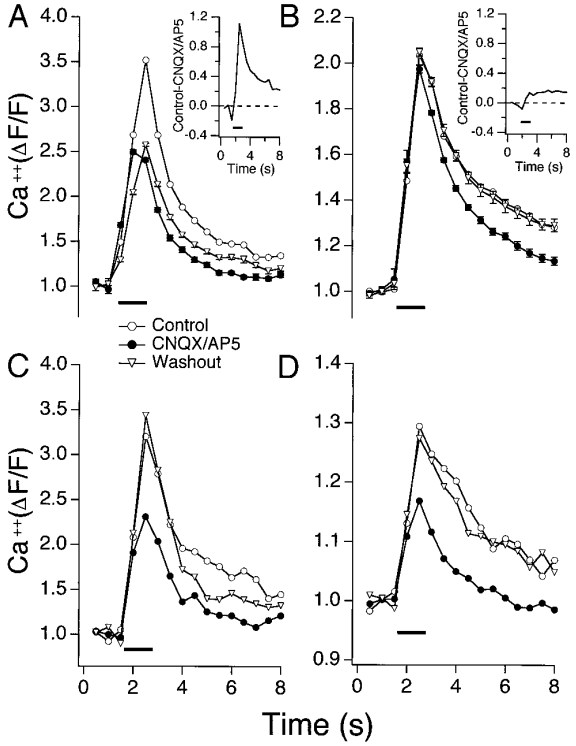

FIG. 4. Effect of the ionotropic glutamate receptor antagonists 6-cyano-7-nitroquinoxaline-2,3-dione (CNQX) and D,L−2-amino-5-phosphonopentanoate (D,L-AP5) on tetanus-induced Ca^{2+} transients. *A*: summary graph of the effect of CNQX (10 μM) and D,L-AP5 (100 μM) on the tetanus-induced (bar; 50 Hz for 1 s; 1.0 ms/stimulus) Ca^{2+} response in reticulospinal dendrites that have been retrogradely labeled with dextran-conjugated calcium-sensitive dyes ($n = 12$). *Inset*: difference between the dendritic fluorescence response to tetanus in the control and CNQX/D,L-AP5 trials. *B*: summary graph of the effect of CNQX (10 μM) and D,L-AP5 (100 μM) on the tetanus-induced (bar) Ca^{2+} response in vestibulospinal axons that have been retrogradely labeled with dextran-conjugated calcium-sensitive dyes ($n = 18$). *Inset*: difference between the axonal fluorescence response to tetanus in the control and CNQX/D,L-AP5 trials. Error bars are SE. normalized to the control response and are often smaller than the symbols. *C*: example of a single experiment showing Ca^{2+} response in reticulospinal dendrites. Note there is a complete washout of CNQX/D,L-AP5. *D*: example of a single experiment showing Ca^{2+} response in vestibulospinal axons. Note there is a complete washout of CNQX/D,L-AP5.

receptors in Ca^{2+} dynamics at the vestibulospinal-reticulospinal synapse. The bath application of the AMPA receptor antagonist CNQX (10 μM, a concentration that has no effect on NMDA-mediated responses in the lamprey) (Alford and Grillner 1990) caused a reversible reduction in the mean peak (to 70 ± 6% of control; $P < 0.05$) dendritic Ca^{2+} transient in response to tetanus; there was also a statistically insignificant reduction in the tail of the dendritic Ca^{2+} signal ($n = 5$). Addition of the NMDA receptor antagonist D,L-AP5 (100 μM) to the superfusate caused an additional decrease in the fluorescence signal. In those experiments ($n = 4$) where D,L-AP5 was applied in the presence of CNQX, the mean peak Ca^{2+} response was reversibly reduced (from 69 ± 5% of control to 30 ± 4% of control; $P < 0.01$); similarly, the mean tail response was decreased (from 78 ± 6% to 23 ± 8% of control; $P < 0.01$). The majority of experiments were performed with the addition of a cocktail of CNQX (10 μM) and D,L-AP5 (100 μM) to the bath. In these experiments ($n = 12$), the mean peak and tail dendritic responses were reduced to 56 ± 2% ($P < 0.01$) and 37 ± 3% ($P < 0.01$) of control, respectively, by the addition of the ionotropic glutamate receptor antagonists (Fig. 4*A*). Although the pooled data shows only partial washout of CNQX and D,L-AP5, some individual experiments did show complete recovery of the Ca^{2+} signal (e.g., Fig. 4*C*).

Antagonists of NMDA and AMPA receptors also had an effect on presynaptic Ca^{2+} dynamics. The application of these compounds caused a reversible reduction in the mean peak tetanic response to 90 ± 1% of control ($P < 0.05$), and a decrease to 49 ± 2% of control ($P < 0.01$) in the mean tail fluorescence transient (Fig. 4*B; n* = 18). Application of CNQX alone caused a statistically insignificant decrease in the peak response to tetanus in the vestibulospinal axons, whereas it reduced the mean fluorescence response in the tail to 66 ± 4% of control ($n = 4$; $P < 0.05$). Although the ionotropic receptor antagonists reduced both axonal and dendritic Ca^{2+} entry, their effects were seen with different kinetics on either side of the synapse. Figure 4, *insets*, shows the subtraction of the mean response in CNQX and D,L-AP5 from the mean control response for both dendrites (4*A; n* = 12) and axons (4*B; n* = 18). CNQX and D,L-AP5 have

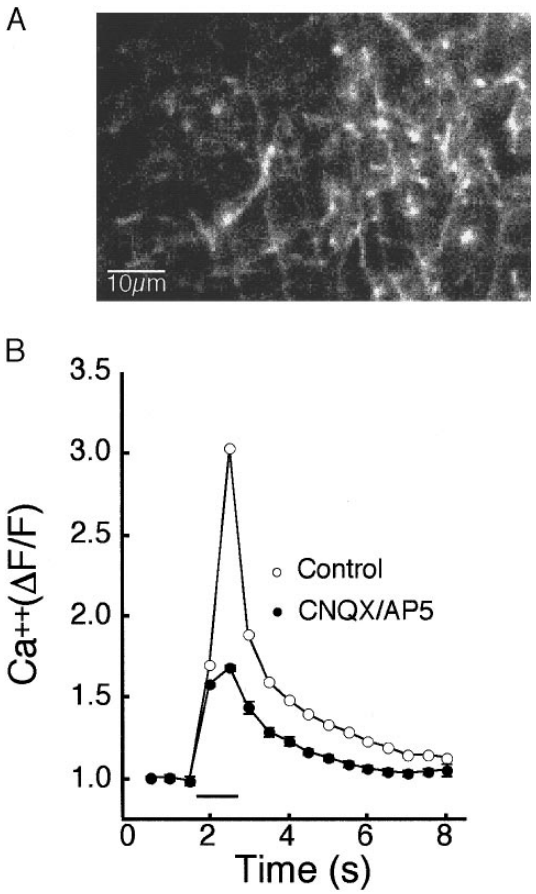

FIG. 5. Reticulospinal dendrites retrogradely labeled in isolation with dextran-conjugated calcium-sensitive dyes *A*: an example of a PRRN dendritic field selectively labeled by the application of dye (Oregon Green 488 BAPTA-1 dextran) to the spinal lateral tracts (see Fig. 1). *B*: pooled data ($n = 4$) of the control and CNQX (10 μM)/D,L-AP5 (100 μM) Ca^{2+} responses to tetanus (bar; 50 Hz for 1 s; 1.0 ms/stimulus) in reticulospinal dendrites dye-filled in isolation. Error bars are SE normalized to the control response and are often smaller than the symbols.

the largest effect in decreasing Ca^{2+} entry into the dendrites during and shortly after the tetanic stimulus, whereas Ca^{2+} entry into the axons is reduced by these antagonists throughout the tetanus and for the entire duration of the trial (~5.5 s posttetanus). Both the pre- and postsynaptic Ca^{2+} responses were completely abolished by TTX (1 μM; $n = 8$).

Postsynaptic responses in selectively labeled reticulospinal dendrites

It is possible that putative presynaptic Ca^{2+} transients recorded from vestibulospinal axons could be ''contaminated'' by postsynaptic transients from reticulospinal dendrites, and vice versa, when both pre- and postsynaptic components contribute to the fluorescence signal. The more medial course in the spinal cord of the descending vestibulospinal axons compared with the reticulospinal axons allows for the selective labeling of either the pre- or postsynaptic elements of the synapse of interest. Experiments were performed in which only the postsynaptic components of the vestibulospinal-reticulospinal synapse, the PRRN somata and dendrites, were retrogradely labeled (e.g., Fig. 5*A*). Results were similar to those experiments in which the entire brain stem was filled. In this case, the mean tail of the Ca^{2+} response was reduced to 43 ± 4% of control (Fig. 5*B; n* = 4) in CNQX and D,L-AP5 versus 36 ± 3% of control ($n = 8$) when the dendrites were not filled in isolation; the difference in these two cases is not statistically significant.

Numerous en passant synaptic contacts are made onto lateral (distal) dendrites of reticulospinal neurons of the PRRN by ipsilateral descending vestibulospinal axons of the nOMI. Conversely, synapses are made by contralateral descending fibers from the more caudal nOMP onto medial (proximal) dendrites of these PRRN cells (Rovainen 1979) (Fig. 6*B*). Previous work has demonstrated that LTP of these vestibular inputs is pathway specific (Alford et al. 1995). To see if rises in synaptically activated dendritic Ca^{2+} correspond with the known locations of the vestibular inputs, fluorescence transients in proximal and distal dendritic trees were compared when either ipsilateral (nOMI) or contralateral (nOMP) tetani were given to vestibulospinal axons. Figure 6*C* shows an example of Ca^{2+} responses in the distal dendrites of the PRRN to tetanic input of either the contralateral nOMP or the ipsilateral nOMI pathways; the fluorescence transient is significantly larger when the tetanic input is given to the pathway that synapses locally on the imaged portion of dendrites. Similarly, a larger Ca^{2+} transient is recorded in the proximal dendrites when the contralateral (nOMP) pathway is tetanized compared with the ipsilateral (nOMI) one (Fig. 6*A*). No significant calcium signal could be seen in PRRN somata in response to tetanic input. In summary, the mean Ca^{2+} transient was significantly larger (peak: $\Delta F/F = 2.23 \pm 0.16$ compared with 1.57 ± 0.11; $P < 0.01$; tail: $\Delta F/F = 1.18 \pm 0.02$ compared with 1.09 ± 0.01; $P < 0.01$; $n = 9$) when the response to stimulation of the different vestibulospinal pathways was matched to their regions of synaptic contact within the dendritic tree.

Presynaptic responses in selectively labeled vestibulospinal axon terminals

As demonstrated above for the dendrites, the presynaptic axons were selectively labeled. The time course, magnitude, and sensitivity to applied pharmacological agents of the fluorescence responses in selectively labeled axons (e.g., Fig. 7*A*) were similar to those found in the experiments using

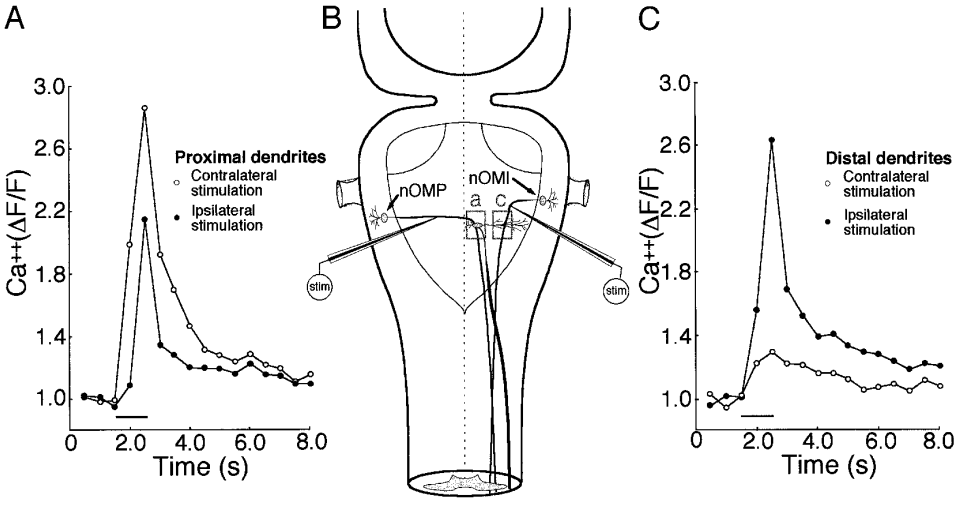

FIG. 6. Rises in postsynaptic Ca^{2+} correspond with the locations of synaptic inputs within the dendritic tree of reticulospinal cells. Experiments were performed in preparations where reticulospinal dendrites of PRRN cells were retrogradely labeled in isolation (see METHODS and Fig. 1) with Oregon Green 488 BAPTA-1 dextran. Experimental setup is shown in *B*. Tetanic stimulations were to vestibulospinal axons of either the contralateral nucleus octavomotorii posterior (nOMP; Stim electrode on *left*) or the ipsilateral nOMI (Stim electrode on *right*). Images were taken from either the proximal dendrites (*A*) or the distal dendrites (*C*) of the reticulospinal cells of the PRRN. Note that the contralateral nOMP axons make synapses on dendrites below (ventral) and lateral to the PRRN somata. *a*: example of an experiment in which the same field of proximal dendrites was imaged during tetanic stimulation (bar; 15.0 μA; 50 Hz for 1 s; 1.0 ms/stimulus) of the contralateral nOMP pathway and the ipsilateral nOMI pathway. *C*: example of an experiment (same cell as used in *A*) in which the same field of distal dendrites was imaged during tetanic stimulation (bar) of the contralateral nOMP pathway and the ipsilateral nOMI pathway. Locations of the stimulating electrode are the same as in *A*.

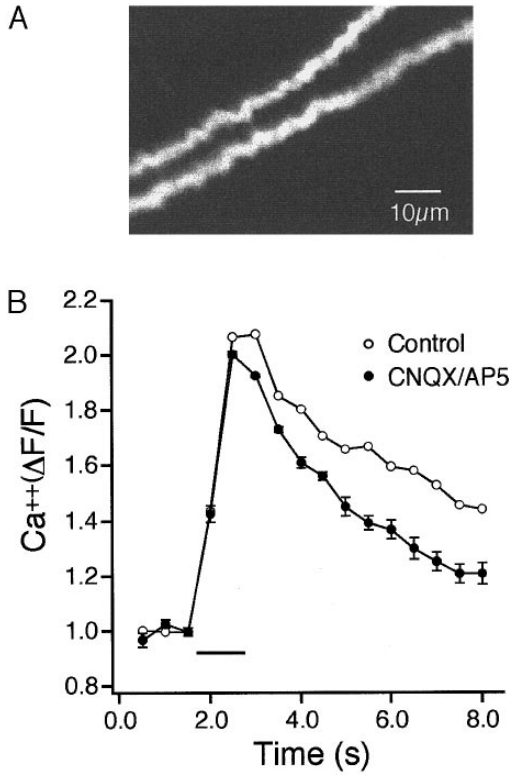

FIG. 7. Response of axons dye-loaded in isolation to tetanic stimulation and the application of ionotropic glutamate receptor antagonists I. *A*: example of 2 axons selectively labeled by the application of dye (Oregon Green 488 BAPTA-1 dextran) to the spinal medial tracts (see Fig. 1). Midline is toward the *bottom;* rostral is toward the *right. B*: pooled data ($n = 7$) of the control and CNQX (10 μM)/D,L-AP5 (100 μM) Ca^{2+} responses to tetanus (50 Hz for 1 s; 1.0 ms/stimulus) in vestibulospinal axons retrogradely labeled in isolation. Bar represents the 1 s tetanus applied to the vestibulospinal axons.

whole brain stem dye-loading. The ionotropic glutamate receptor antagonists CNQX and D,L-AP5 caused a decrease in mean fluorescence to 47 ± 4% of control as measured at the tail of the transient in response to tetanic stimulation (Fig. 7*B; n* = 7), similar to the decrease (52 ± 1% of control; $n = 11$) for preparations where the entire brain stem was dye-loaded.

The selective labeling technique therefore was used to investigate the receptor mechanisms underlying part of the presynaptic signal in more detail. Tetanus-evoked Ca^{2+} transients were recorded in individually labeled vestibulospinal axons. CNQX (10 μM) reduced the mean tetanus-evoked calcium response at the peak to 80 ± 7% and at the tail to 61 ± 4% of the control amplitude (Fig. 8*Ai*; $n = 7$). In the continued presence of CNQX, Mg^{2+} was washed from the superfusate to alleviate its voltage-dependent blockade of NMDA receptors. Tetanic stimulation caused a fluorescence transient that exceeded the amplitude of the control response; the mean response at peak and tail was increased to 134 ± 9% and 150 ± 4% of control, respectively. Subsequent application of D,L-AP5 (100 μM) eliminated the enhancement seen in Mg^{2+}-free Ringer, causing a reduction in the mean amplitude of the response to 82 ± 6% of the peak control response and to 58 ± 5% of the tail control response (Fig. 8*Aii*).

The mean data hide a variability in the response of the axonal Ca^{2+} transients that was quite marked. An example is given from a single field of data in Fig. 8, *B* and *C*. Tetanic stimulation led to Ca^{2+} transients in two axons in this field. In one axon (Fig. 8*Bi*), the application of CNQX (10 μM) caused little or no change in amplitude of the transient, whereas removal of Mg^{2+} enhanced the response only slightly (Fig. 8*Bii*). In the second axon, the small transient was abolished by the application of CNQX in normal saline (Fig. 8*Ci*). Subsequent wash-out of Mg^{2+} revealed a large component that was eliminated by the addition of D,L-AP5 (100 μM); restoring the superfusate to normal Ringer allowed recovery of the response to the small control amplitude (Fig. 8*Cii*).

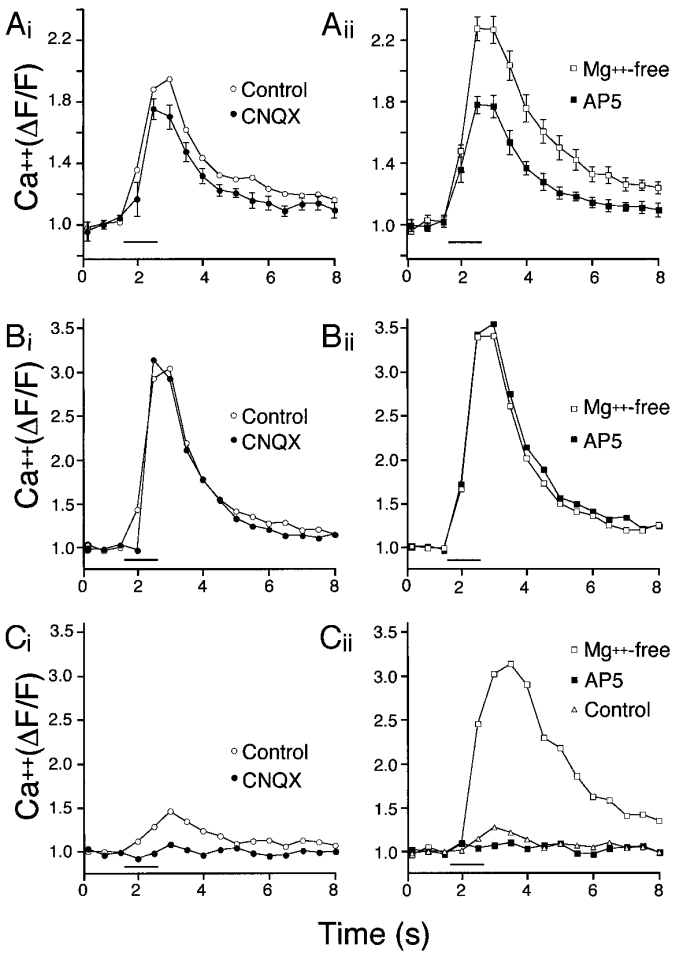

FIG. 8. Response of axons dye-loaded in isolation to tetanic stimulation and the application of ionotropic glutamate receptor antagonists II. *A*: pooled data from all experiments done with Mg^{2+}-free protocol ($n = 7$). *Ai*: axonal Ca^{2+} transient evoked by tetanus before (○) and after (●) the addition of CNQX. *Aii*: same response after wash-out of Mg^{2+} (□) from the saline and then the addition of 100 μM D,L-AP5 (■). *B*: example of an axon in which neither CNQX (10 μM; *Bi*) nor the wash-out of extracellular Mg^{2+} had a substantial effect on presynaptic Ca^{2+} entry. Symbols same as in *A*. *C*: in the same sequence of antagonist applications and stimuli a different axon in the same field demonstrates a markedly different response, whereby CNQX eliminated the response in normal saline (*Ci*) and D,L-AP5 eliminated a large response that was evoked after wash-out of Mg^{2+} from the superfusate (*Cii*). All symbols are the same as *A* but wash to control conditions (△) also is shown in *Cii*. In all experiments, a tetanus (bar) of 50 Hz for 1 s (1.0 ms/stimulus) was given.

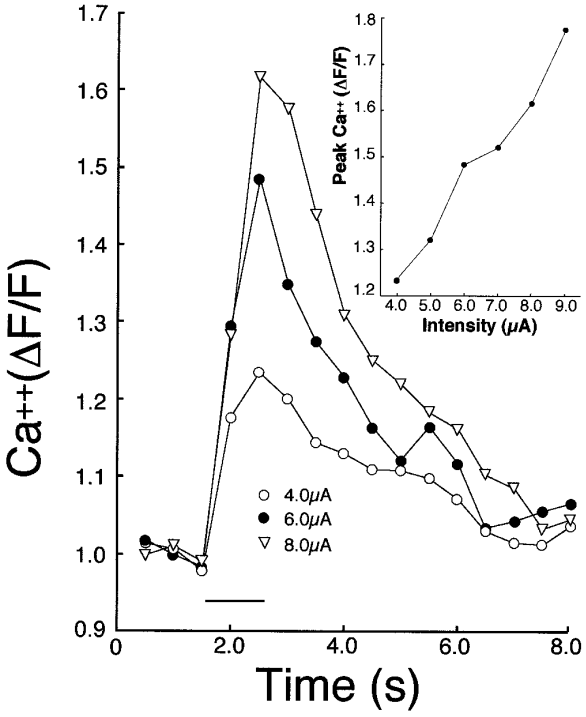

FIG. 9. Recruitment of excitatory inputs onto the presynaptic element. Representative Ca^{2+} signals from an experiment in which the extracellular stimulus intensity of the tetanic input (50 Hz for 1 s; 1.0 ms/stimulus) was progressively increased. Bar represents the 1 s tetanus given to the vestibulospinal axons. *Inset*: graph of the peak Ca^{2+} ($\Delta F/F$) vs. stimulus intensity for the single axon shown in the main graph.

Consistent with the finding that presynaptic Ca^{2+} dynamics are affected by ionotropic glutamate receptors, transients within a given individual axon were increased progressively with greater stimulus intensities. These experiments were performed in preparations where progressively larger stimulus intensities (between 5.0 and 18.0 μA; 50 Hz for 1 s; 1.0 ms/stimulus) were applied to the presynaptic fibers. The possibility that direct electrotonic depolarization of the axons by the electrode was responsible for the effect on presynaptic Ca^{2+} signals was ruled out, as the fluorescence signal always was eliminated by TTX (1 μM). An example of such an experiment ($n = 5$) is shown in Fig. 9.

Electrophysiology of presynaptic vestibulospinal axons

To confirm whether axo-axonic inputs to the vestibulospinal axons may have been responsible for the CNQX- and D,L-AP5–sensitive components of the presynaptic Ca^{2+} transient, microelectrode recordings were made from vestibulospinal axons at the level of the PRRN dendrites. Stimuli were applied to the vestibular pathways as for the imaging experiments. Axons were identified as vestibulospinal by two means: *1*) extracellular stimulation of the vestibulospinal tracts in the brain stem led to short latency (less than discernible from the stimulus artifact; <2 ms) action potentials in the recorded axon (Fig. 10*A*) and *2*) axons were filled by pressure ejection through the recording pipette with dextran-conjugated fluorescein. Subsequent imaging revealed axons passing through the region of the PRRN to the spinal cord in one direction and to the location of the ipsilateral nOMI in the other. In all cases ($n = 4$), reducing the single stimulus intensity to subthreshold for action potential initiation revealed a depolarizing event; this was largely blocked by application of CNQX (10 μM; $n = 2$; Fig. 10*A*, *inset*). Suprathreshold tetanic stimulation of these axons revealed a train of action potentials (1 per stimulus) superimposed on a plateau potential with an amplitude that ranged from 3 to 10 mV ($n = 4$; Fig. 10*B*).

Effect of bath applications of the agonists NMDA, AMPA, and kainate

Bath applications of ionotropic glutamate receptor agonists were carried out in combination with Ca^{2+} imaging to confirm the presence of these receptors presynaptically. Perfusions of NMDA (100 μM), AMPA (10 μM), and kainate (10 μM) were performed on preparations in which the vestibulospinal axons were retrogradely labeled in isolation. Agonists were added in the presence of 1 μM TTX. A

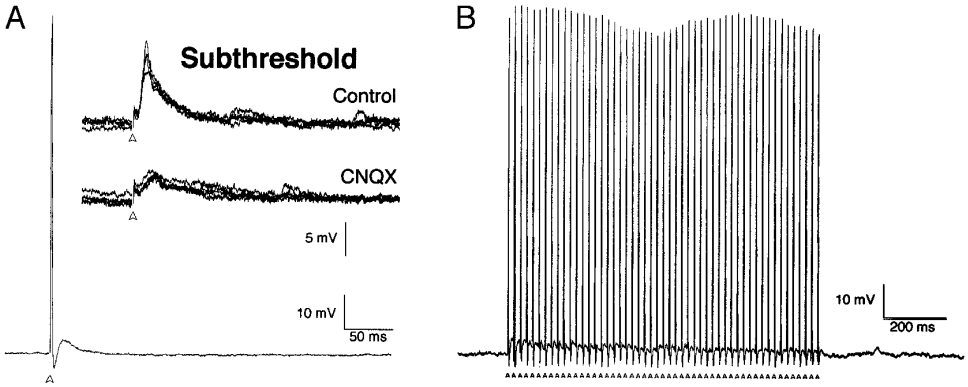

FIG. 10. Electrophysiological recording from a vestibulospinal axon. *A*: vestibular axon is stimulated (arrowhead) to evoke an action potential by a single stimulus (12 μA, 1.0 ms) to the vestibular pathway. *Top inset*: response to stimulation at the same location but at a lower intensity (6 μA). Responses to 4 such stimuli at 10 s intervals are overlaid. *Bottom inset*: responses to a stimulus of the same intensity in the presence of CNQX (10 μM). Again the responses to four sequential stimuli are overlaid. *B*: response in the axon to a tetanus of 50 stimuli in 1 s (1.0 ms/stimulus) at the higher stimulus intensity (12 μA). A spike is evoked at each stimulus (arrowheads). Note that the response is raised on a plateau of depolarization.

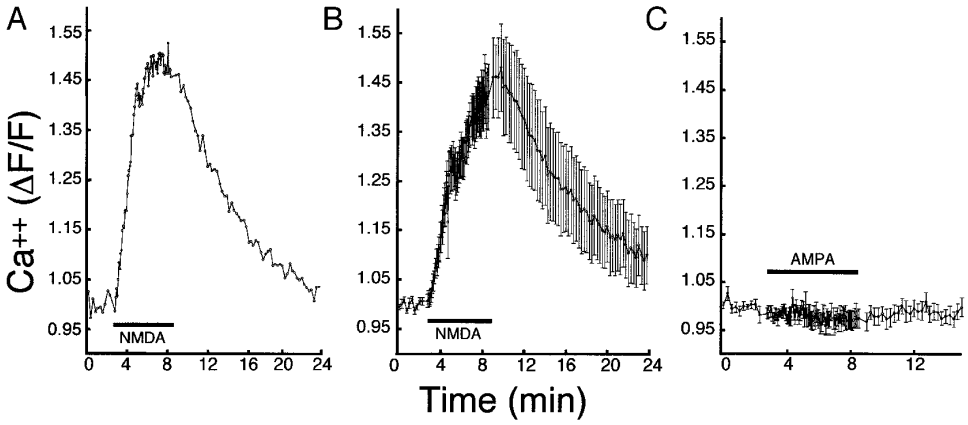

FIG. 11. Bath applications of the ionotropic glutamate receptor agonists NMDA and α-amino-3-hydroxy-5-methyl-4-isoxazolepropionic acid (AMPA). Vestibulospinal axons were retrogradely labeled in isolation (see Fig. 1) with Oregon Green 488 BAPTA-1 dextran. Bar represents the agonist wash-in period. *A*: example of the presynaptic calcium response to a wash-in of 100 μM NMDA in the presence of 1 μM tetrodotoxin (TTX). *B*: pooled data (n = 13 axons) of experiments where NMDA (100 μM) and TTX (1 μM) were bath-applied. *C*: pooled data (n = 10 axons) of experiments where AMPA (10 μM) and TTX (1 μM) were bath-applied.

representative example of an NMDA wash-in from a single vestibulospinal axon is shown in Fig. 11*A*. Presynaptic Ca^{2+} levels rise abruptly at the start of NMDA wash-in and fall off toward baseline with a slower time course during agonist wash-out. Figure 11*B* shows the mean response of 13 axons (gathered from 2 identical trials) to the wash-in of NMDA in TTX. In all cases (n = 22 axons), NMDA caused a rapid and reversible increase in axonal fluorescence. Bath-application of AMPA (in the presence of 1 μM TTX) caused no discernible rise in presynaptic Ca^{2+} (Fig. 11*C; n* = 10 axons). Concomitant addition of cyclothiazide (100 μM), a compound that prevents AMPA receptor desensitization in other vertebrate preparations (Patneau et al. 1993; Yamada and Tang 1993), and AMPA had no effect on increasing the presynaptic fluorescence transient (n = 8 axons). Likewise, kainate was ineffective in increasing presynaptic $[Ca^{2+}]_i$ (n = 6 axons).

DISCUSSION

This study demonstrates that presynaptic activation of ionotropic glutamate receptors occurs after stimulation of the vestibulospinal axons in the lamprey, and this activation leads to Ca^{2+} entry in addition to that evoked by action potential invasion of the terminal. Such receptor activation on presynaptic elements has been reported in several preparations. Lamprey spinal cord reticulospinal axon terminals receive excitatory glutamatergic inputs impinging on presynaptic receptors (Cochilla and Alford 1997). NMDA receptors have been shown to be present on presynaptic terminals in the mammalian hippocampus (Smirnova et al. 1993), amygdala (Farb et al. 1995), and the bed nucleus of the stria terminalis (Gracy and Pickel 1995). There is also evidence for presynaptic AMPA (Barnes et al. 1994; Ginsberg et al. 1995) and kainate (Dev et al. 1996) receptors in a variety of preparations. In this study, the function of pre- and postsynaptic ionotropic glutamate receptors was studied using calcium-sensitive dyes; some discussion of the efficacy of the Ca^{2+} imaging technique follows.

Use of calcium-sensitive dyes

Calcium-sensitive dyes are buffers with a limited dynamic range defined by their Ca^{2+} affinity. Our goal was to record transients in subsynaptic elements while not interfering significantly with calcium-dependent physiological processes. Neurotransmitter release follows Ca^{2+} binding to presynaptic proteins with low affinities (Augustine and Neher 1992; Augustine et al. 1991), such that Ca^{2+} concentrations of at least tens of micromolar are required for triggering release (Llinas et al. 1992). High-affinity dyes will compromise these mechanisms should the dye concentration rise to compete with endogenous intracellular Ca^{2+} buffers. In these studies, the dye loaded into the presynaptic terminals did not prevent release; a robust transmitter-dependent response always was recorded in the postsynaptic dendrites whether or not the presynaptic elements were loaded with dye. Additionally, we have demonstrated that dye concentration in the axon terminal is low (~2 μM). This concentration of Fura-2 (a dye with similar affinity to those used here) would not compete effectively with endogenous buffers involved in release (Neher and Augustine 1992). The use of dextran-conjugated dyes has the further advantage of immobilizing the dye by binding to cellular proteins and thus will not break down spatial calcium gradients.

The small size of most vertebrate presynaptic terminals precludes the use of high-affinity dyes for recording the events readily observed in this study. Optical resolution of structures much less than 0.5-μm apart is not feasible. This inability to resolve diffusional distances has the consequence that saturating concentrations of Ca^{2+} are recorded throughout the structure (Tank et al. 1995). This is less of a problem in invertebrate giant synapses (Augustine et al. 1991; Delaney et al. 1989) and in large axons of the vertebrate lamprey. We have used 500 Hz sampling to show that the axonal Ca^{2+} response measured from individual vestibulospinal axons sums with repetitive stimulation. Thus the dye is not saturated by Ca^{2+} entry at the presynaptic element. Although it is not possible to quantitate Ca^{2+} concentrations with the dyes and protocols used in these experiments, changes in fluorescence provide a powerful comparative tool for the study of Ca^{2+} dynamics.

Electrical stimulation and spiking of the axon leads to Ca^{2+} entry through VOCCs responsible for transmitter release. The Ca^{2+} concentration in the vicinity of the channel is extreme (as high as 300 μM) (Llinas et al. 1992). If low-affinity binding proteins of the release machinery are located close to the channels, their requirement for high $[Ca^{2+}]_i$ may be met readily. Two factors preclude the measurement of Ca^{2+} transients directly responsible for release in this study. The time course of these transients is rapid compared

with the sampling rates attainable here. Even at 500 Hz, initial fluorescence changes cannot be resolved. Second, the Ca^{2+} affinities of the dyes used here are too high to detect Ca^{2+} concentrations in the tens to hundreds of micromolar range. Calcium entering the axon from the extracellular space diffuses from the plasmalemma along a steep concentration gradient; further, the local $[Ca^{2+}]_i$ falls as Ca^{2+} is buffered by endogenous proteins. In addition to VOCC-activated Ca^{2+} entry, presynaptic receptor-mediated events affect Ca^{2+} dynamics. These processes occur over various time scales such that $[Ca^{2+}]_i$ often takes seconds to return to baseline after stimulation (Bacskai et al. 1995). It is the dynamics of this residual Ca^{2+} that is reflected by the signals recorded in these experiments. The goal of these studies was to investigate various sources and pharmacological properties of these transients on both sides of the synapse.

Presynaptic calcium transients and ionotropic glutamate receptors

Tetanic stimulation evokes a Ca^{2+} transient in presynaptic vestibulospinal axons which far outlasts the tetanus. During stimulation of the axon, Ca^{2+} will enter through VOCCs after the passage of each action potential through the presynaptic element of the en passant synapse. The maintained fluorescence signal may have a number of sources: calcium, from voltage-gated ionophores, may diffuse from the plasma membrane into the axon; it may be released from internal stores themselves activated by this voltage-gated Ca^{2+} entry or by presynaptic autoreceptors. Interestingly, a further source of Ca^{2+} contributes to the recorded signal in these studies. Increasing the stimulus intensity of the tetanus, without altering the frequency, duration, or number of applied stimuli, leads to a graded increase in the fluorescence signal in single identified axons. The stimulus-induced response was eliminated by the application of TTX to the preparation, implying that the response was not due to a direct depolarization of the axon from the stimulating electrode. The most parsimonious conclusion is that stimulation of the vestibulospinal pathway activates axo-axonic synaptic inputs, which can lead either directly to Ca^{2+} entry or that may enhance action potential-induced Ca^{2+} entry. The variability of tetanically induced presynaptic calcium transients, and their sensitivity to glutamate receptor antagonists and Mg^{2+}-free Ringer (e.g., Fig. 8), supports this conclusion. The exact placement of the extracellular stimulating electrode, in conjunction with the specific location along the axon that is chosen for imaging, will have a profound effect on the measured signals. For instance, if only a single vestibulospinal axon is stimulated and this particular axon is imaged, the transient will be dominated by Ca^{2+} entry through VOCCs and thus will be insensitive to CNQX and D,L-AP5. The more likely case that occurred in these experiments is that the stimulating electrode activates multiple vestibulospinal fibers, some of which make excitatory axo-axonic synapses onto the imaged axon, and the resulting signal is due in part to glutamate receptor activation.

Evidence for presynaptic ionotropic glutamate receptors in the brain stem also is provided by the observation that CNQX and D,L-AP5 significantly reduce the tetanus-induced Ca^{2+} entry into the presynaptic element and that the D,L-AP5–sensitive component of this response is highly magnesium dependent. Although it is possible that activation of postsynaptic excitatory amino acid receptors could lead to a buildup of extracellular K^+, which in turn could cause voltage-dependent Ca^{2+} entry into presynaptic axons via the indirect depolarization of these processes, the rapid time course of the ionotropic glutamate receptor-modulated electrophysiological response (Fig. 10*A*) weighs against this as a likely mechanism. As these axons have been shown to receive excitatory axo-axonic inputs, the indirect effects would have to take place within micro- to milliseconds to account for the antagonist sensitivity of the excitatory postsynaptic potentials. Furthermore, there is only a slight depolarization in these axons (plateau) in response to the tetanic input (Fig. 10*B*). Other work in our laboratory has indicated that there are no low-voltage–activated (T-type) VOCCs present on lamprey axons (A. J. Cochilla and S. Alford, unpublished observation).

Some vestibulospinal-reticulospinal synapses comprise an electrical component in addition to fast glutamatergic chemical components (Alford and Dubuc 1993). The possibility exists that depolarization of postsynaptic reticulospinal cells could result in the depolarization of presynaptic vestibulospinal axons via these gap junctions; this in turn could lead to Ca^{2+} entry through VOCCs. The existence of such a phenomenon might suggest that the pharmacological sensitivity of the presynaptic calcium signals could be mediated through an indirect (postsynaptic) mechanism. Paired recordings obtained from vestibulospinal axons and reticulospinal dendrites have demonstrated that the electrical components of excitatory postsynaptic currents in PRRN cells, in response to the spiking of a single presynaptic vestibulospinal axon, are on the order of 50 pA (Schwartz and Alford 1997). Given an average action potential amplitude of 120 mV, a gap junction conductance of ~400 pS can be calculated. Assuming a large postsynaptic depolarization of 20 mV, one that is consistent with either the depolarization seen in response to tetanus (Alford et al. 1995) or the bath-application of NMDA (N. E. Schwartz and S. Alford, unpublished observation) and an axonal input impedance of 100 MΩ, a presynaptic gap junction-mediated depolarization of 0.8 mV can be calculated. This would not be expected to contribute significantly to calcium entry through VOCCs in this preparation. A similar analysis has been performed on reticulospinal neurons in the lamprey spinal cord (Cochilla and Alford 1997).

It also was demonstrated that bath-application of NMDA (in TTX) leads to a rapid and reversible increase in axonal Ca^{2+}, providing strong evidence for the existence of NMDA receptors capable of modulating presynaptic calcium. The absence of an effect of exogenous AMPA is more difficult to interpret. Although calcium-permeable AMPA receptors are present in mammals (Hollmann et al. 1991), most subtypes of AMPA receptors are calcium impermeant. The effect of CNQX on presynaptic Ca^{2+} entry with tetanus may indicate that AMPA receptor-mediated effects augment voltage-dependent Ca^{2+} entry. As such, insufficient depolarization during the AMPA/TTX wash-ins may have precluded the entry of calcium—and any modulation by AMPA receptor activation—through VOCCs. Furthermore, AMPA receptors rapidly desensitize in the presence of agonist (Trus-

sell and Fischbach 1989). Although coapplication of cyclothiazide, a compound that prevents AMPA receptor desensitization in mammalian systems (Patneau et al. 1993; Yamada and Tang 1993), was without effect, the efficacy of this compound has not been investigated in the lamprey. The lack of effect of kainate suggests that this subtype of non-NMDA receptors are not responsible for mediating the CNQX-sensitive calcium transients.

Origins of postsynaptic calcium transients

Tetanic stimulation of the lamprey vestibulospinal system evokes a Ca^{2+} transient in the postsynaptic elements of the vestibulospinal-reticulospinal synapse. This signal is reduced but not eliminated by the application of antagonists to NMDA and AMPA receptors. Although there is some overlap in location of synaptic inputs onto these neurons from contralateral (nOMP) and ipsilateral (nOMI) sources, a good correlation is seen between the known locations of synaptic inputs and the localized amplitudes of the Ca^{2+} transients. The significant component of the tetanus-evoked postsynaptic Ca^{2+} rise present after the coapplication of NMDA and AMPA receptor antagonists may be due to postsynaptic VOCC activation and/or the activation of metabotropic glutamate receptors (Frenguelli et al. 1993). This is a subject for further investigation.

Conclusions

Prolonged increases in $[Ca^{2+}]_i$ (several milliseconds to seconds) mediate changes responsible for phenomena of synaptic plasticity (Malenka et al. 1992). We have recorded prolonged Ca^{2+} signals in response to a LTP-inducing input on both sides of a glutamatergic synapse. Both pre- and postsynaptically, these signals are sensitive to ionotropic glutamate receptor antagonists. The presynaptic transients are due, in part, to the activation of excitatory axo-axonic synapses onto vestibulospinal axons. Our results do not exclude the possibility of a postsynaptically generated retrograde messenger causing a rise in presynaptic calcium; however, the existence of presynaptic NMDA receptors capable of modulating Ca^{2+} homeostasis highlights the role of receptor-mediated processes in plasticity on both sides of the vertebrate synapse.

We thank Drs. N. Traverse Slater and Amanda J. Cochilla for comments on the manuscript and A. Jha for assistance with anatomic tracing.

This work was supported by National Institute of Neurological Disorders and Stroke Grant RO1 NS-32114.

Address for reprint requests: S. Alford, Dept. of Physiology, M-211, Northwestern University Medical School, 303 East Chicago Ave., Chicago, Illinois 60611.

Received 22 August 1997; accepted in final form 22 December 1997.

REFERENCES

ALFORD, S. AND DUBUC, R. Glutamate metabotropic receptor mediated depression of synaptic inputs to lamprey reticulospinal neurons. *Brain Res.* 605: 175–180, 1993.

ALFORD, S., FRENGUELLI, B. G., SCHOFIELD, J. G., AND COLLINGRIDGE, G. L. Characterisation of Ca^{2+} signals induced in hippocampal CA1 neurones by the synaptic activation of NMDA receptors. *J. Physiol. (Lond.)* 469: 693–716, 1993.

ALFORD, S. AND GRILLNER, S. CNQX and DNQX block non-NMDA synaptic transmission but not NMDA-evoked locomotion in lamprey spinal cord. *Brain Res.* 506: 297–302, 1990.

ALFORD, S., ZOMPA, I., AND DUBUC, R. Long-term potentiation of glutamatergic pathways in the lamprey brainstem. *J. Neurosci.* 15: 7528–7538, 1995.

AUGUSTINE, G. J., ADLER, E. M., AND CHARLTON, M. P. The calcium signal for transmitter secretion from presynaptic nerve terminals. *Ann. NY Acad. Sci.* 635: 365–381, 1991.

AUGUSTINE, G. J. AND NEHER, E. Calcium requirements for secretion in bovine chromaffin cells. *J. Physiol. (Lond.)* 450: 247–271, 1992.

BACSKAI, B. J., WALLÉN, P., LEV-RAM, V., GRILLNER, S., AND TSIEN, R. Y. Activity-related calcium dynamics in lamprey motoneurons as revealed by video-rate confocal microscopy. *Neuron* 14: 19–28, 1995.

BARNES, J. M., DEV, K. K., AND HENLEY, J. M. Cyclothiazide unmasks AMPA-evoked stimulation of [^{3}H]-L-glutamate release from rat hippocampal synaptosomes. *Br. J. Pharmacol.* 113: 339–341, 1994.

BEKKERS, J. M. AND STEVENS C, F. Presynaptic mechanism for long-term potentiation in the hippocampus. *Nature* 346: 724–729, 1990.

BLISS, T.V.P. AND COLLINGRIDGE, G. L. A synaptic model of memory: long-term potentiation in the hippocampus. *Nature* 361: 31–39, 1993.

BLISS, T.V.P. AND LØMO, T. Long-lasting potentiation of synaptic transmission in the dentate area of the anaesthetised rabbit following stimulation of the perforant path. *J. Physiol. (Lond.)* 232: 331–356, 1973.

BUCHANAN, J. T., BRODIN, L., DALE, N., AND GRILLNER, S. Reticulospinal neurons activate excitatory amino acid receptors. *Brain Res.* 408: 321–325, 1987.

COCHILLA, A. J. AND ALFORD, S. Glutamate receptor-mediated synaptic excitation in axons of the lamprey. *J. Physiol. (Lond.)* 499: 443–457, 1997.

COLLINGRIDGE, G. L., KEHL, S. J., AND MCLENNAN, H. Excitatory amino acids in synaptic transmission in the Schaffer collateral-commissural pathway of the rat hippocampus. *J. Physiol. (Lond.)* 334: 33–46, 1983.

COLLINGRIDGE, G. L. AND LESTER, R.A.J. Excitatory amino acid receptors in the vertebrate central nervous system. *Pharmacol. Rev.* 41: 143–210, 1989.

DALE, N. AND GRILLNER, S. Dual component synaptic potentials in the lamprey mediated by excitatory amino acid receptors. *J. Neurosci.* 6: 2653–2661, 1986.

DELANEY, K. R., ZUCKER, R. S., AND TANK, D. W. Calcium in motor nerve terminals associated with posttetanic potentiation. *J. Neurosci.* 9: 3558–3567, 1989.

DELIAGINA, G., ORLOVSKY, G. N., GRILLNER, S., AND WALLÉN, P. Vestibular control of swimming in lamprey. II. Characteristics of spatial sensitivity of reticulospinal neurons. *Exp. Brain Res.* 90: 489–498, 1992a.

DELIAGINA, G., ORLOVSKY, G. N., GRILLNER, S., AND WALLÉN, P. Vestibular control of swimming in lamprey. III. Activity of vestibular afferents: convergence of vestibular inputs on reticulospinal neurons. *Exp. Brain Res.* 90: 499–507, 1992b.

DEV, K. K., BARNES, J. M., COLLINGRIDGE, G. L., AND HENLEY, J. M. Regulation of glutamate release by presynaptic kainate receptors in the hippocampus. *Nature* 379: 78–81, 1996.

EBERHARD, M. AND ERNE, P. Calcium binding to fluorescent calcium indicators: calcium green, calcium orange and calcium crimson. *Biochem. Biophys. Res. Commun.* 180: 209–215, 1991.

FARB, C. R., AOKI, C., AND LEDOUX J. E. Differential localization of NMDA and AMPA receptor subunits in the lateral and basal nuclei of the amygdala: a light and electron microscopic study. *J. Comp. Neurol.* 362: 86–108, 1995.

FRENGUELLI, B. G., POTIER, B., SLATER, N. T., ALFORD, S., AND COLLINGRIDGE, G. L. Metabotropic glutamate receptors and calcium signaling in dendrites of hippocampal CA1 neurones. *Neuropharmacology* 32: 1229–1237, 1993.

GINSBERG, S. D., PRICE, D. L., BLACKSTONE, C. D., HUGANIR, R. L., AND MARTIN, L. J. The AMPA glutamate receptor GluR3 is enriched in oxytocinergic magnocellular neurons and is localized at synapses. *Neuroscience* 65: 563–575, 1995.

GRACY, K. N. AND PICKEL, V. M. Comparative ultrastructural localization of the NMDAR1 glutamate receptor in the rat basolateral amygdala and bed nucleus of the stria terminalis. *J. Comp. Neurol.* 362: 71–85, 1995.

HOLLMANN, M., HARTLEY, M., AND HEINEMANN, S. Ca^{2+} permeability of KA-AMPA-gated glutamate receptor channels depends on subunit composition. *Science* 252: 851–853, 1991.

IRIKI, A., PAVLIDES, C., KELLER, A., AND ASANUMA, H. Long-term potentiation in the motor cortex. *Science* 245: 1385–1387, 1989.

KIMURA, F., NISHIGORI, A., SHIROKAWA, T., AND TSUMOTO, T. Long-term potentiation and *N*-methyl-D-aspartate receptors in the visual cortex of young rats. *J. Physiol. (Lond.)* 414: 125–144, 1989.

KULLMANN, D. M. AND NICOLL, R. A. Long-term potentiation is associated with increases in quantal content and quantal amplitude. *Nature* 357: 240–244, 1992.

LLINAS, R., SUGIMORI, M., AND SILVER, R. B. Microdomains of high calcium concentration in a pre-synaptic terminal. *Science* 256: 677–679, 1992.

LYNCH, G., LARSON, J., KELSO, S., BARRIONUEVO, G., AND SCHOTTLER, F. Intracellular injections of EGTA block induction of hippocampal long-term potentiation. *Nature* 305: 719–721, 1983.

MALENKA, R. C., LANCASTER, B., AND ZUCKER, R. S. Temporal limits on the rise in postsynaptic calcium required for the induction of long-term potentiation. *Neuron* 9: 121–128, 1992.

MALENKA, R. C. AND NICOLL, R. A. NMDA-receptor-dependent synaptic plasticity: multiple forms and mechanisms. *Trends Neurosci.* 16: 521–527, 1993.

MALINOW, R. AND TSIEN, R. W. Presynaptic enhancement shown by whole-cell recordings of long-term potentiation in hippocampal slices. *Nature* 346: 177–180, 1990.

MCCLELLAN, A. D., MCPHERSON, D., AND O'DONOVAN, M. J. Combined retrograde labeling and calcium imaging in spinal cord and brainstem neurons of the lamprey. *Brain Res.* 663: 61–68, 1994.

NEHER, E. AND AUGUSTINE, G. J. Calcium gradients and buffers in bovine chromaffin cells. *J. Physiol. (Lond.)* 450: 273–301, 1992.

NICOLL, R. A. AND MALENKA, R. C. Contrasting properties of two forms of long-term potentiation in the hippocampus. *Nature* 377: 115–118, 1995.

O'DELL, T. J., HAWKINS, R. D., KANDEL, E. R., AND ARANCIO, O. Tests of the roles of two diffusible substances in long-term potentiation: evidence for nitric oxide as a possible early retrograde messenger. *Proc. Natl. Acad. Sci. USA* 88: 11285–11289, 1991.

OHTA, Y. AND GRILLNER, S. Monosynaptic excitatory amino acid transmission from the posterior rhombencephalic reticular nucleus to spinal neurons involved in the control of locomotion in lamprey. *J. Neurophysiol.* 62: 1079–1089, 1989.

ORLOVSKY, G. N., DELIAGINA, T. G., AND WALLÉN, P. Vestibular control of swimming in lamprey I. Responses of reticulospinal neurons to roll and pitch. *Exp. Brain Res.* 90: 479–488, 1992.

PATNEAU, D. K., VYKLICKY, L., JR., AND MAYER, M. L. Hippocampal neurons exhibit cyclothiazide-sensitive rapidly desensitizing responses to kainate. *J. Neurosci.* 13: 3496–3509, 1993.

POCKETT, S. AND FIGUROV, A. Long-term potentiation and depression in the ventral horn of rat spinal cord in vitro. *Neuroreport* 4: 97–99, 1993.

RANDIC, M., JIANG, M. C., AND CERNE, R. Long-term potentiation and long-term depression of primary afferent neurotransmission in the rat spinal cord. *J. Neurosci.* 13: 5228–5241, 1993.

ROVAINEN, C. M. Synaptic interactions of reticulospinal neurons and nerve cells in the spinal cord of the sea lamprey. *J. Comp. Neurol.* 154: 207–223, 1974.

ROVAINEN, C. M. Electrophysiology of vestibulospinal and vestibuloreticulospinal systems in lampreys. *J. Neurophysiol.* 42: 745–766, 1979.

SCHLATTERER, C., KNOLL, G., AND MALCHOW, D. Intracellular calcium during chemotaxis of *Dictyostelium discoideum*: a new fura-2 derivative avoids sequestration of the indicator and allows long-term calcium measurements. *Eur. J. Cell Biol.* 58: 172–181, 1992.

SCHWARTZ, N. E. AND ALFORD, S. Pre-synaptic activation of mGluRs activates the spontaneous release of transmitter at a glutamatergic synapse. *Soc. Neurosci. Abstr.* 23: 2275, 1997.

SCHWARTZ, N. E., DUBUC, R., AND ALFORD, S. Calcium dependence of LTP induction by postsynaptic glutamate metabotropic receptors in the brainstem. *Soc. Neurosci. Abstr.* 21: 601, 1995.

SCHWARTZ, N. E., HOLT, A. J., AND ALFORD, S. Presynaptic calcium dynamics at a plastic glutamatergic synapse. *Soc. Neurosci. Abstr.* 22: 1240, 1996.

SHUPLIAKOV, O., BRODIN, L., CULLHEIM, S., OTTERSEN, O. P., AND STORM-MATHISEN, J. Immunogold quantification of glutamate in two types of excitatory synapse with different firing patterns. *J. Neurosci.* 12: 3789–3803, 1992.

SMIRNOVA, T., LAROCHE, S., ERRINGTON, M. L., HICKS, A. A., BLISS, T.V.P., AND MALLET, J. Transsynaptic expression of a presynaptic glutamate receptor during hippocampal long-term potentiation. *Science* 262: 433–436, 1993.

STEVENS, C. F. AND WANG, Y. Reversal of long-term potentiation by inhibitors of haem oxygenase. *Nature* 364: 147–149, 1993.

TANK, D. W., REGEHR, W. G., AND DELANEY, K. R. A quantitative analysis of presynaptic calcium dynamics that contribute to short-term enhancement. *J. Neurosci.* 15: 7940–7952, 1995.

TRUSSELL, L. O. AND FISCHBACH, G. D. Glutamate receptor desensitization and its role in synaptic transmission. *Neuron* 3: 209–218, 1989.

WICKELGREN, W. O. Physiological and anatomical characteristics of reticulospinal neurones in lamprey. *J. Physiol. (Lond.)* 270: 89–114, 1977.

WILLIAMS, J. H., ERRINGTON, M. L., LYNCH, M. A., AND BLISS, T.V.P. Arachidonic acid induces a long-term activity-dependent enhancement of synaptic transmission in the hippocampus. *Nature* 341: 739–742, 1989.

YAMADA, K. A. AND TANG, C. M. Benzothiadiazides inhibit rapid glutamate receptor desensitization and enhance glutamatergic synaptic currents. *J. Neurosci.* 13: 3904–3915, 1993.